Facile synthesis of few layer graphene from bituminous coal and its application towards electrochemical sensing of caffeine

E. Senthil Kumar[1], V. Sivasankar[2], R. Sureshbabu[3], S. Raghu[2]*, R. A. Kalaivani[1]*

[1]*Department of Chemistry, Vels University, Chennai, 600117, India*
[2]*Vels Advanced Energy Research Centre, Vels University, Chennai, 600117, India*
[3]*Centro Federal de Educação Tecnológica, Celso Suckow da Fonseca, Rio de Janeiro, 20271110, Brazil*

*Corresponding author, Tel: (+91) 44 - 2266 2500 / 2501-3; E-mail: rakvani@yahoo.co.in; subraghu_0612@yahoo.co.in

Abstract

A simple, cost-effective, sensitive and highly selective method for the detection of caffeine has been developed at graphene modified carbon paste electrodes (GME). We synthesis of graphene oxide (GO) derived from bituminous coal by improved modified Hummers method. The synthesized graphene were characterized by UV-Visible Spectroscopy, FT-IR and Raman Spectroscopy, X-ray Diffraction Studies, Field Emission Scanning Electron Microscopy (FE-SEM) and High Resolution Transmission Electron Microscopy (HR-TEM). An electrochemical behavior of caffeine at the coal derived from graphene modified electrode was investigated by cyclic voltammetry (CV) and chronoamperometry (CA). By way of a result, graphene modified electrode (GME) showed good electrocatalytic activity towards the oxidation of caffeine. Under the optimized tentative conditions, caffeine was sensed in the concentration range from 0.2 to120 µmol L^{-1} with a detection limit of 90 nm molL^{-1} at a signal-to-noise ratio = 3. Hence, the graphene modified electrode (GME) could be used for the determination of caffeine in soft-drinks samples with high sensitivity and good selectivity. In this chronoamperometry shows a high catalytic currents are desirable for applications such as use in sensors. Copyright © 2017 VBRI Press.

Keywords: Bituminous coal, few–layer graphene, carbon paste electrode and cyclic voltammetry, chronoamperometry.

Introduction

Coal may be a good source to replace graphite as the raw materials since it is inexpensive and plentiful. The structure of coal is quite complexes **[1-3]**, its simplified composition contains angstron or nanometer-sized crystalline carbon domains with defects that are linked by aliphatic amorphous carbon. Coal is still mainly used as an energy source, in contrast to crystalline carbon allotropes such as fullerenes, graphene, graphite and diamond that have found applications in electronics, physics, chemistry and biology **[4-7]**. However research on the chemistry of coal has been reported earlier **[8-9]**. Further essentially, the coal is molecular solid which has incompact structure while graphite is a lattice solid without weak bonds, so the process can be simplified and some of the hazardous chemicals can be avoided. Chemical exfoliation is an effective way of producing graphene in large quantity. Synthesized graphene quantum dots from bituminous coal has already been reported **[10-16]**, and also various carbon based materials including graphite or graphite oxide, carbon nanotubes and carbon fibres has been prepared **[17-20]**. The morphology of the three types of carbon materials is different originating from the different structure of coals. As a novel two dimensional carbon nanomaterials,

graphene has attracted tremendous scientific attention in recent years due to its outstanding physical and chemical properties. Facile synthesis of one-step wet chemical route to fabricate a graphene quantum dots from their three types of coal: anthracite, bituminous coal, and coke. Various carbon sources, including graphite, hydrocarbons (CH_4, C_2H_2), polymer, natural biomaterials (food, insects) and even plastic waste have been widely used for synthesizing of graphene. However, as the natural most plentiful carbon source in the world, coal has not been investigated for the production of graphene up to now. Tomita et al. evaluated the size of graphene sheets in several chinese anthracites by a temperature programmed oxidation method **[21]**. A single layer of graphene atoms in a hexagonal lattice, has currently concerned much attention due to its novel electronic and mechanical properties **[36-38]**. Graphene is usually prepared by the reduction of its graphene oxide, a typical pseudo-two-dimensional oxygen-containing solid form, possesses functional groups such as hydroxyls, epoxides, and carboxyls. Thus, by combining extraordinary mechanical properties and low costs, graphene or graphene oxide sheets are expected to promising nanoscale filler for the next generation of nano-composite materials. Its exhibit enormously high thermal conductivity, good mechanical strength, high mobility of charge carrier, high specific

surface area, quantum hall effect, and outstanding electric conductivity. Graphene materials were fabricating various electrical devices, e.g., field-effect transistor, batteries, ultra-sensitive sensors, electromechanical resonators, and electrochemical biosensors. Caffeine has many physiological effects and such as gastric acid secretion dieresis, and stimulation of the human central nervous system [22]. It's widely used for plant products and beverages. The IUPAC name of caffeine is 3, 7-dihydro-1, 3, 7-trimethyl-1H-purine-2, 6-dione **(Fig. S1)** and it's an active alkaloid compound in coffee, cola nuts, cocoa beans, tea leaves. It can cause an adverse mutation effect when excessively consumed, various inhibition of DNA repair and cyclic AMP phosphodiesteraseactivity [23-24], cancer, heart diseases and complicated in pregnant women and aging [26-27]. Different methods have been developed for the determination of caffeine [29], such as UV spectrophotometry, mass spectroscopy and FTIR spectrophotometry, thin layer chromatography, gas chromatography and high performance liquid chromatography, capillary electrophoresis [30-33]. Normally, the above methods are costly, time consuming sample pretreatment are required and difficult. Electrochemical methods are displayed by luxury characteristic, such as ease, high sensitivity and easy to use [25-28], have been developed for the determination of caffeine. In this area of electrochemical sensor, researcher are uses of various materials like physio-chemical properties, because they provide a high surface area and improve the bio-compatibility, stability and immobilization of biomolecules on the electrode surface. The carbon paste electrode (CPE) were primarily started in 1958 by Adams and most of the researchers, are wide variety of modifying such as polymers, enzymes and nanomaterials have been developed. Carbon paste electrodes (CPE) are used in application of electrochemical studies and analysis. Its shows very low background current, low cost, easy to prepare, simple surface renewal process [34-36]. The chemically modified electrode (CMEs) have been usually used for the sensitive and selective systematic technique to detection of (qualitative & quantitative) micro level in the biological important compounds.

Recently graphene based materials has been possess an excellent electrochemical catalytic activities and should be considered as a modified material electrode with excellent performance of sensors [30-32]. In this present study to synthesize of graphene derived from bituminous coal and investigated the electrochemical sensitivity of caffeine detection. In this method we prove a easy, consistent, and inexpensive way for the examine of caffeine in the soft-drink samples at low levels. Here we report graphene from bituminous coal in large quantity by a new solution phase technique.

Experimental

Materials

Coal (bituminous coal) and caffeine, (99%) were purchased from Sigma-Aldrich. Sodium Nitrate, Potassium Permanganate, ammonia was obtained from E. Merck. All these chemicals were of analytical reagent grade and throughout all the experiments, ultra-pure water was used.

Synthesis

According to earlier reports, synthesis of graphene oxide was prepared from bituminous coal by well-known Hummers method with little modification [37-38]. In short- term, 2 g bituminous coal powder was added into a 250 ml beaker, then 1 g $NaNO_3$ and 46 ml H_2SO_4 were added into it sequentially under stirring in 24 hrs. Then the mixture was further stirred for 6hrs at 80°C. When the temperature was reduced to room temperature, the solution was diluted by 1M HNO_3 and GO was getting a sedimentation by centrifugation at 7200 RPM for 10 min, and the obtained powder was washed with warm water until the pH valueof the upper layer suspension arrives at near 7. A solution GO was obtained after dissolving the sedimentation in the aqueous ammonia. For the solution on piranha was cleaned quartz surfaces. Finally thermal treatment was taken under argon flow at 900 °C for 5hrs and the graphene was obtained. **Fig. 1.** Systematic representation of graphene from bituminous coal.

Characterizations

UV-visible spectra were measured with Perkin Elmer Lambda 25 UV-vis Spectrometer. FT-IR spectra (KBr pellets) were recorded using a BRUKER IFS 66/S instrument. Wide-angle X-ray diffraction (XRD) analyses were carried out by exploying X-ray diffractometer (D/MAX-1200, RigakuDenki Co. Ltd., Japan). The X-ray diffraction patterns with Cu Ka radiation (λ= 1.5406) at 40 kV and 100 mA were recorded in the range of 2θ= 5-70°. For the XRD measurement, the sample was prepared by freeze-drying of the hydrogel,
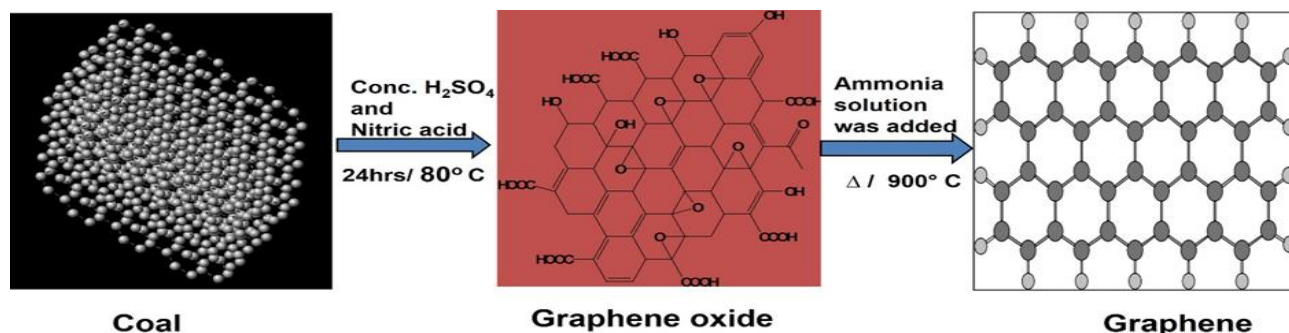
Fig. 1. Systematic representation of graphene derived from bituminous coal

further it was crushed into a fine powder. The Raman spectrums were recorded by raman spectroscopy and the excitation wavelength was 534 nm. The morphology and elemental composition of the synthesized graphene were observed by Scanning Electron Microscope (Hitachi S-3400 N). High resolution transmission electron microscopy (HR-TEM) FEI, TECHNAI 2300 kV. Cyclic voltammetry (CV) and Chronoamperometry measurements were carried out by using a CHI 760D electrochemical workstation (CH instrument USA). Carbon paste electrode and its modified electrodes were used as working electrode. A Pt wire served as the counter electrode and an Ag/AgCl (in saturated KCl solution) was used as the reference electrode. Cyclic voltammograms (CVs) were obtained by immersing the GME in caffeine standard solution and scanning in the potential range from 0.8 V to 1.6 V vs Ag/AgCl. Upon completion of each scan, the modified electrode was placed in a blank buffer solution and cyclic scan was continued until no unwanted noise peak comes out, then the electrode was washed with water and dried with filter for use.

### Fabrications of electrode

The graphene modified electrode (GME) was prepared by mixing 900 mg of graphite powder and 100 mg of graphene and using a mortar and pestle. A syringe was used to add silicon oil to the mixture, which was mixed well for 40 min, until a homogeneously wetted paste, was obtained. The paste was then packed into a glass tube electrical contact was made by pushing a copper wire down the glass tube into the back of the mixture. When necessary, a new surface was obtained by pushing an excess of the paste out of the tube and polishing it on a weighing paper. The obtained electrode was noted as graphene modified/CPE (GME), graphene oxide/CPE (GOME) and bare (CPE) are represented respectively and prepared with same procedure.

Results and discussion

Functional analyses

Fig. 2a shows UV-visible spectra of graphene oxides in water an absorption peak at 230 nm with a shoulder at 300 nm corresponding to the π-π* transition due to the aromatic C-C bonds and the n-π transition due to the C=O bonds respectively. After GO reduced by a thermal treatment to obtained an graphene and its formation of absorption peak at ~ 280 nm. Bituminous coal [39], graphene oxide (GO) and graphene (GR) were characterized by FT-IR an exposed in **Fig. 2b**. The FT-IR spectrum of graphene oxide, board peak at 3425 cm^{-1} was initiate from stretching vibrations of hydroxyl groups. The C-O-H deformation of carboxyl groups (-COOH) was observed at 1734 cm^{-1}. The skeletal vibrations of unoxidized graphitic domains were observed around 1621 cm^{-1}. The band at 1410, 1210 and 1050cm^{-1} are corresponding to C-O-H deformation C-OH is stretching expoxyl groups and C-O is stretching vibration (alkoxy groups) respectively. Similar to a earlier report in the literature **[38, 39]** as well as the FT-IR

spectrum of reduced graphene oxide shows that the oxygen containing functional groups was almost removed after the reduction process. The reduction process due to the band at 1568 cm^{-1} corresponds to the skeletal vibration of RGO sheets which agrees with earlier reports **[38]**. The peak at 1261 cm^{-1} shows that the partial presence of functional groups and its indicate the oxygen containing functional groups was reduced by thermal treatment.
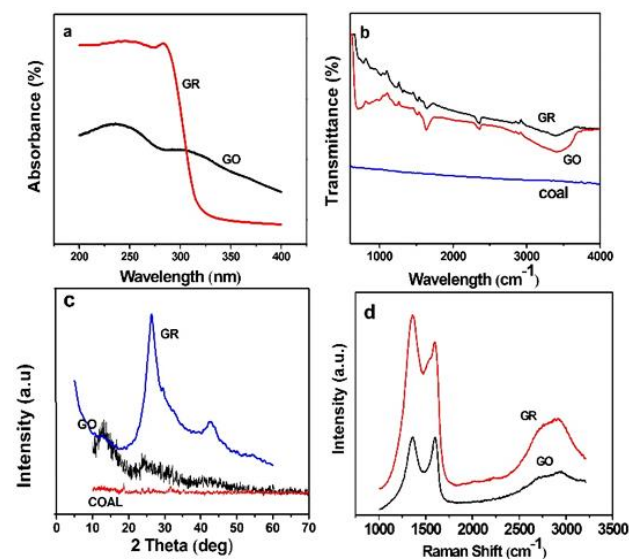
Fig. 2(a). UV-visible spectra of graphene oxide and graphene. **(b)**. FITR spectrum of a) bituminous coal, b) graphene oxide and c) graphene. **(c)**. XRD pattern of bituminous coal, GO, and graphene (GR). **(d)**. Raman spectra of the D and G bands of GO and graphene (GR).

Structural analyses

The XRD patterns of reduced graphene oxide and GO were shown in **Fig. 2c**. The characteristic XRD peak of graphene oxide, appeared value at $2\theta = 11.3°$ **[40-41]** and its has interlayer distance corresponding to 0.8 nm, the oxidation treatment of bituminous coal. It shows that a laminar structure with the higher the d-spacing is observed in graphene oxide. That means it could be attributed to the presence of epoxy, carbonyl and other functional groups. This evidence to show that coal is converted into graphene oxide. $2\theta=25.01°$, the d spacing indicates the distance of graphite layers have been efficiently increased during the thermal, expansion process to be occurs and its corresponding interlayer distance decrease from 0.8 nm was 0.43nm. In raman spectrum of graphene oxide and graphene are shown in **Fig. 2d**. They exhibited the two raman peaks at about 1580 and 1348 cm^{-1}, corresponding to G and D bands, respectively. The G bands represented as the tangential vibration of carbon atoms in the graphite carbon layers, while the D band indicates the presence of the disordered carbon atoms. Compared with GO (1588 cm^{-1}), the G bands for the graphene sheets is sharper and shifts to lower frequency (1584 cm^{-1}). The ratio of D and G band intensity (I_D/I_G) decrease from 1.73 to 1.30, which means an increases in the degree of graphitization of graphene sheets. Eventhough an thermal expansion and reduction occurs, to remove the most of the oxygen-containing

groups from the graphene oxide, these method cannot repair an hole and defects within the carbon structure completely. The raman spectrum of graphene sheets are indicates a huge imperfection and defects present in the carbon sheets. Bituminous coal derived graphene oxide to be reduced thermally at 900 °C to get graphene.

Morphological analyses

In **Fig 3. (a,b)** show as morphology of graphene in FESEM and **(c, d)** HR- TEM image.The reduced graphene oxide shows that the wrinkled like structure of stable and transparent graphene sheets on the copper grid. During the oxidation process wrinkled stuctured graphene oxide sheets are formed. Further, thermal reduction process, graphene sheets still exist wrinkled sheets closely associated with each other forming.
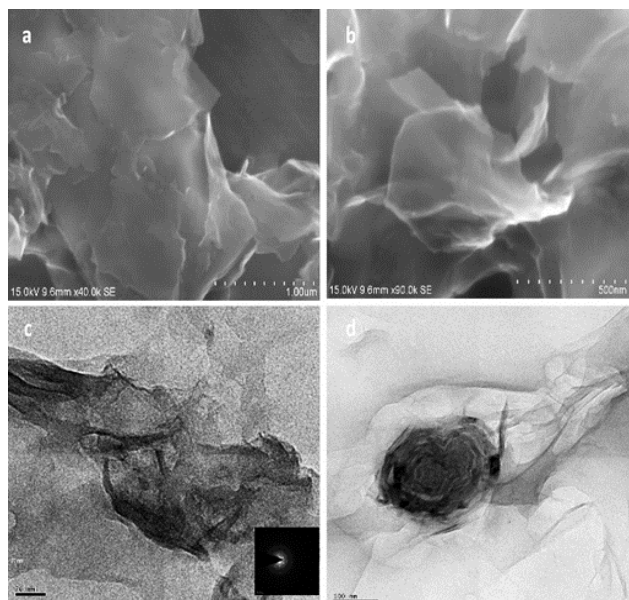
Fig. 3. (a-b) FESEM image of graphene at different magnifications. (c- d) HR-TEM image of graphene at diffraction. (Insert image shows the diffraction pattern).

Electrochemical analyses

Initially we investigate the effect of supporting electrolyte on the electrochemical sensitivity of the prepared electrodes. CVs of the GME in the presence of 1.0×10^{-5} M caffeine in 0.01 M different supporting electrolytes including sulfuric acid, nitric acid, acetic acid and hydrochloric acid. The potential of peak current, caffeine is closely related to the pH of the electrolyte solution. For the determination of the effect of pH value on the sensor response, different pH values was investigated by CVs. So that pH 2.0 was chosen for this cyclic voltammetry as reported studies.

Cyclic voltammetry analysis of modified electrodes

According to the various supporting electrolytes which are highest sensor response was obtained in 0.01M sulfuric acid and to be chosen in the supporting electrolyte. In cyclic voltammograms (CVs) at the bare (CPE), GOME and GME in 0.01M H_2SO_4 (pH.2) solution containing 1.0×10^{-5} M caffeine are shown in **Fig. 4a**.

While no anodic peak of caffeine appeared in bare electrode. However an anodic peak was obviously appeared on GOME (I_{pa}= 2.631 µA) and GME appeared at (I_{pa} = 4.14 µA) electrode. The oxidation peak current was higher at the GME than the GOME and bare (CPE). Without addition of caffeine the GOME and GME anodic peak current were appeared at (I_{pa} = 2.6µA and 4.14µA) scan rate of 50 mVs^{-1} are respectively **(Fig.4b)**. Noticebly higher the anodic peak current with addition of caffeine (Ipa =3.2µA and 6.11µA) were found GOMEand GME in the medium containing in 0.01 M H_2SO_4 (pH 2.0); at a scan rate of 50 mVs^{-1} **(Fig. 4b)**.
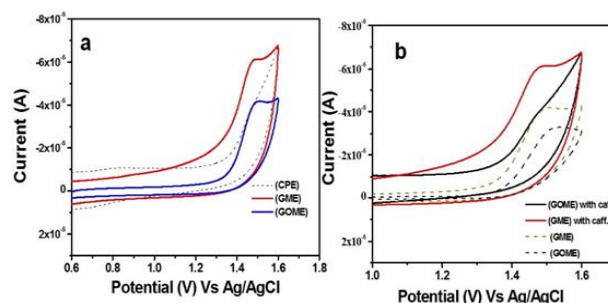
Fig. 4. (a) CVs at the bare (CPE), GOME and GME in 0.01M H_2SO_4 (pH.2) solution. (b). CVs of caffeine (1.0×10^{-5}molL^{-1}) at the GOME, GME in 0.01M H_2SO_4 solution with scan rate at 50 mV s^{-1}.

Electrochemical behaviour of caffeine

Fig. 5a shows the influence of different scan rates on the current responses of the GME in the presence of 1.0×10^{-5} M caffeine.The Randle equation to identify the reversible process of the modified electrodes in the caffeine detection as follows;

$$ip = 2.69 \times 10^5 \, An^{3}/_{2} \, D^{1}/_{2} \, cv^{1}/_{2} \qquad (1)$$

where, i_p refers to the peak current, and A is the area of electrode (cm^2), and n is the number of electron transferred, D is the diffusion coefficient, C is the concentration and υ is the scan rate. The linearly proportional of anodic peak currents to the square root of the scan rate in the range from 5 mV to 500 mV, whereas the linear regression equation was expressed as a I_{pa}= 0.891x + 0.159 R = 0.998 (I_{pa} in µA, υ in Vs-1, R=0.998), suggesting the GME undergoes an diffusion controlled process. According to Randles equation (1), the diffusion coefficient of caffeine was calculated and found to be 3.03. When the scan rate to be increase, the anodic peak potential at the GME was positively shifted slightly. To an irreversible system, E_{pa} and ln v should submit to the equation at higher scan rate.

$$Epa = \left(E + \frac{RT}{(1-\alpha)nF} x \left\{ 0.780 + \frac{\ln(D_R{}^{1}/_{2})}{K^0} \right) + \right.$$
$$\left. \ln \left[\frac{(1-\alpha)nFv}{RT} \right] {}^{1}/_{2} \right\} \qquad (2)$$

In this studies, Epa = 0.053x + 1.422 R = 0.998 **(Fig. S2)**. Only oxidation peaks were observed, indicating that the oxidation of caffeine was a totally irreversible electrode process. Along with the increase of the scan

rate, the oxidation peak currents of caffeine increased gradually, and the relationship of the oxidation peak current with the square root of the scan rate were established with linear regression equations (Eqn. (2)). **Fig. 5b** shows the addition of analyte was investigated by the cyclic voltammetry using GME. From the CV results caffeine onset of oxidation peak potential was observed from 1.48V to 1.5V vs Ag/AgCl. The anodic peak current significantly increases from 5.483×10^{-7}A to 4.184×10^{-6} A, with addition of caffeine concentration in the range of 0--2μmolL-1 respectively. Among the CV results , shows an excellent and better electrochemical performance was found in GME compared with GOME than CPE. The electrochemical mechanism of caffeine oxidized on GME is a two electron-transferring irreversible reaction in our GME Fig. 5b. Insert shows the calibration plot of current responses versus concentration of caffeine.
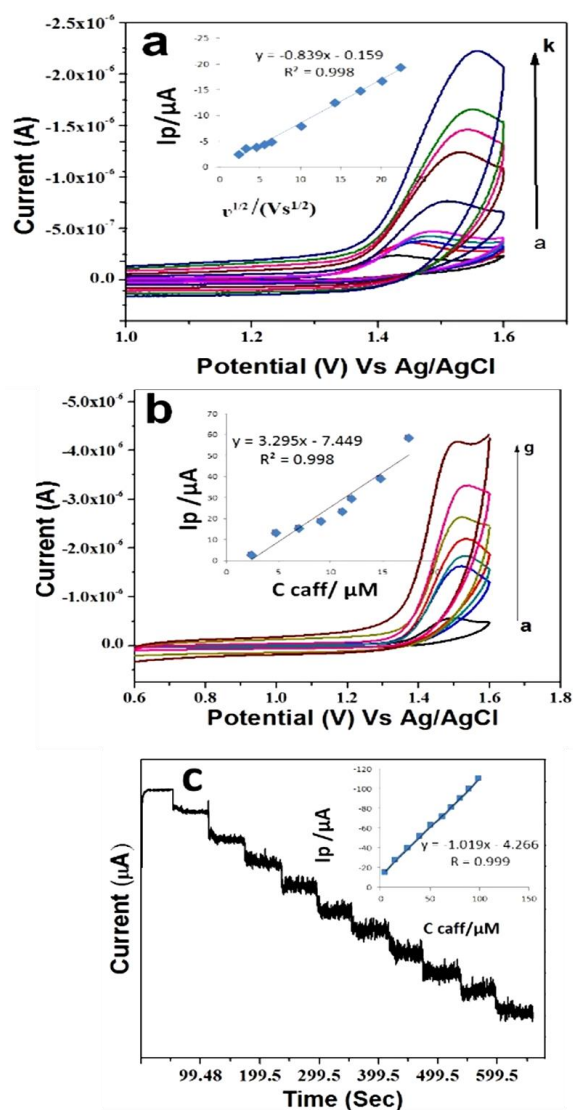
Fig. 5. a CVs of (GME) in the presence of 1.0×10^{-5} M caffeine with different scan rate of 10mV to 500mV. Insert I_{Pa}Vs Sq. rt of scan rates. **5b**. CVs of GME in the presence of 1.0×10^{-5} M caffeine with different addition of (0, 0.2, 0.4, 0.6, 0.8, 1& 2 μml). Insert I_{pa} Vs Sq. rt. of the scan rates. **Fig. 5c**. Amperomertic i-t curve for the determination of caffeine using GME in 0.01M H_2SO_4 (pH-2). Insert the plot for catalytic current Vs concentration.

To evaluate the catalytic rate constant K was investigated by chronoamperometry Fig. 5c. shows an chronoamperograms of GME 0.01M H_2SO_4 solution in the absence and presence of caffeine. It shows that the amperometric response curve of the GME to caffeine determination. The amperometric response of GME has been recorded with the successive addition of caffeine to a continuously stirring background electrolyte at the fixed potential. The fixed potential is 1.5V, the oxidation current increased to reach a stable plateau within 60 seconds with each addition of caffeine into the 0.01 M H_2SO_4 solution. The experimental results shows an amperometric current response is linearly with the concentration of caffeine and the linear equation could be expressed as ipa (μA) $=42.66+1.019$ $C_{caf/\mu M}$, with an correlation coefficient of R=0.999 and the detection limit of caffeine is 3.03, which indicates the good response of the GME for oxidation of caffeine under dynamic condition. A comparison of the different electrochemical methods for the determination of caffeine is summarized in **Table 4.** The method for the determination of caffeine proposed herein shows high sensitivity and a wide linear range, and is suitable to be the most commonly used analytical method for detecting low concentrations of caffeine.

Interference studies

Also we investigate the interference effects of some compounds, a fixed amount of 1.0×10^{-5} M caffeine spiked with various foreign species, such as glucose, glycine, histidine, citric acid, sucrose, fructose,amino acetic acid and L-tyrosine were evaluated under the same experimental conditions. The GME esponses obtained from caffeine was accepted as 100% and compare the sensor responses of other compounds. The results obtained were shows in **Table-1**.

Table 1. Interference studies of the effect – caffeine sensor response.

Interference	Current (μA)*	Current (μA)®	Different current ratio of *®
Glucose	19.61	19.67	0.32
Glycine	—	19.89	1.42
Citric Acid	—	—	19.36
Sucrose	—	19.34	–1.35
Fructose	—	19.85	1.21
Aminoacetic Acid	—	—	20.08
L-Tyrosine	—	20.26	3.31
Catechin	—	20.05	2.26

Real sample analyses

The interference effects of the studied compounds were negligible, which clearly evidence, prove reasonablesensitive and selectivity of caffeine by bituminous coal derived from graphene modified electrode (GME). **Table-2** shows comparison of detection performance of our test sensor and other methods to the real samples analysis. Data were presented as the average of 5 replicates of trials±R.S.D. The results are in agreement with the value by using UV-Visible absorption

spectrophotometry and HPLC as well as the regulation of $I_{pa}(\mu A) = 42.66 + 1.019\, C_{caf/\mu M}$ (R=0.999) in the range of 9.0×10^{-7} to 9.0×10^{-6} M. According to the results it was especially that caffeine in the soft drinks can be sensitively determined with the development method. To test the reliability, a standard addition method was adopted to determine the cola beverage samples spiked with suitable caffeine. The results are shown in table–3. The recoveries were 97.8 to 102%. As results of obtained by using UV-Visible absorption spectrophotometer and HPLC, which revealed a good accuracy of proposed method.

Table 2. Analysis of caffeine in real samples by the UV–Vis spectroscopic, Test sensor and HPLC methods (n = 5).

Sample	Caffeine (mg/ml)		
	Test sensor*	UV-Vis spectroscopic*	HPLC*
Coca cola	0.0997±0.004	0.103±0.0051	0.0991±0.005
Pepsi cola	0.107±0.0053	0.11±0.0046	0.106±0.0049
Energy drink	0.192±0.009	0.187±0.0009	0.19±0.008
Instant coffee	0.1357±0.0112	0.139±0.01	0.1343±0.010
Commercial coffee sample1	0.1762±0.0036	0.1774±0.0019	0.1761±0.003
Commercial coffee sample2	0.1751±0.0031	0.1768±0.0029	0.1756±0.0028

Conclusion

In summary, we prepared graphene oxide and graphene from the bituminous coal by improved modified hummers method, then thermal treatment to obtained graphene. The graphene oxide and graphene were characterized from physio-chemical instrument such as UV-Visible, FTIR and Raman spectroscopy, XRD, FE-SEM and HR-TEM studies were showed the crystalline structure and the morphology of graphene. The GOME and GME were characterized by electrochemical method and its improved sensitivity of caffeine detection. Among the results GME shows excellent electrocatalytic activity for the oxidation of caffeine and sensitivity of the range 5.483×10^{-7}A to 4.184×10^{-6} A and detection of limit is 1.04×10^{-8} A. The GME electrode has the benefit of easy preparation, high stability and sensitivity, also it can be used to the determination of caffeine in commercially available food/other industrial samples.
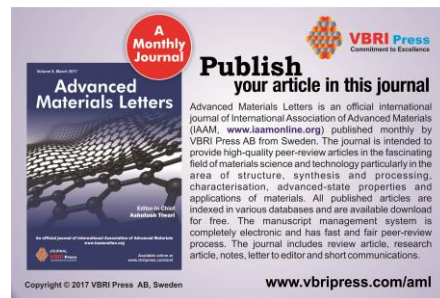
References

1. Given, Peter. H.; Kinetics and Mechanism of Solution of High Volatile Coal; Hill, G. R.; Hariri, H.; Reed, R. I.; Anderson, L. L.; Advance in Chemistry,(Eds.) **1966**, *55*, 427–447.
   DOI: 10.1021/ba-1966-0055.ch027

2. Lakhe, S.B.; Paunikar, W.N.; Parhad, N.M.; Water Research, **2002,** *36*, 13, 3298–3306.
   DOI: 10.1016/S0043-1354(02)00026-X

3. Lu, L.; Sahajwalla, V.; Kong, C.; Harris, D.; Carbon, **2001**, *39* 1821–1833.
   DOI: 10.1016/S0008-6223(00)00318-3

4. Levine, D.G.; Schlosberg, R.H.; Silbernagel, B.G.; Proc. *Natl Acad. Sci.* USA, **1982,** *79*, 3365–3370.
   DOI: 10.1073/pnas.79/10/3365

5. Bakry, R.; Rainer, M.V.; Muhammad, N.H.; Matthias, R.; Zoltan, S.; Christian, W.H.; Günther, K.B.; *Int. J. Nanomed.*, **2007,** *2*, 639–649.
   DOI: 10.1021/acs.nanolett.5b04735

6. Parlak, O.; Tiwari, A.; Turner, APF.; Tiwari, A.; *Biosensors and Bioelectronics*, **2013**, 49, 53.
   DOI: 10.1016/j.bios.2013.04.004

7. Logan, B.; Cheng, S.; Watson, V.; Estadt, G.; *Environ. Sci. Technol.,* **2007**, *41*, 3341–3346.
   DOI: 10.1021/es062644y

8. Anthony, D.B.; Howard, J.B.; *AlChE J.*, **1976**, *22*, 625–656.
   DOI: 10.1002/aic.690220403

9. Sternberg, H.W.;Delle Donne, C.L.; *Fuel*, **1974**, *53*, 172–175.
   DOI: 10.1016/0016-2361(74)90005-2

10. Sun, Y.; Mukherjee, A.; Kuznetsov, O.; Thaner, R.; Alemany, L. B.; Billups, W. E.; *Energy Fuels*, 2011, *25*, 1571–1577.
    DOI: 10.1021/ef200106g

11. Tang, L.; Ji, R.; Li, X.; Teng, K. S.; Lau, S.P.; *Part. Syst. Char.,* **2013**, *30*, 523–531.
    DOI: 10.1002/ppsc.201200131

12. Parlak, O.; Turner, APF.; Tiwari, A.; *Advanced Materials*, **2014**, 26, 482.
    DOI: 10.1002/adma.201303075

13. Pan, D.; Zhang, J.; Li, Z.; Wu, M.; *Adv. Mater*. **2010**, *22*, 734–738.
    DOI: 10.1002/adma.200902825

14. Loh, K.P.; Bao, Q.; Eda, G.; Chowilla, M.; Nat. *Chem*., **2010**, *2*, 1015–1024.
    DOI: 10.1038/nchem.907

15. Shen, J.; Zhu, Y.; Chen, C.; Yang, X.; Li, C.; *Chem. Commun*., **2010**, *47*, 2580–2582.
    DOI: 10.1039/c0cc04812g

16. Feng, Y.; Meilian, Z.; Baozhan, Z.; Dan, X.; Li, W.; Yong, G.; *J. Mater. Chem*., **2012**, *22*, 25471–25479.
    DOI: 10.1039/c2jm35471c

17. Sung, K.; Sung, W.H.; Min-Kook, K.; Dong Yeol, S.; Dong Hee, S.; Chang Oh, K.; Seung Bum, Y.; Jae Hee, P.; Euyheon, H.; Suk-Ho, C.; Geunwoo, K.; Sunghyun, S.; Cheolsoo, S.; Hyoung Joon, C.; Sukang, B.; Byung Hee, H.; *ACS Nano*., **2012**, *6*, 8203–8208.
    DOI: 10.1021/nn302878r

18. Fei, L.; Min-Ho, J.; Hyun Dong, H.; Je-Hyung, K.;Yong-Hoon, C.; Tae Seok. S.; *Adv. Mater*., **2013**, *25*, 3657–3662.
    DOI: 10.1002/adma.201300233

19. Yiqing,S.; Shiqi, L.; Chun, L.; Lei, P.; Yen, W.; Gaoquan, S.; *Phys. Chem. Chem. Phys*. **2013**, *15*, 9907–9913.
    DOI: 10.1039/c3cp50691f

20. Lingling, L.; Gehui, W.; Guohai, Y.; Juan, P.; Jianwei, Z.;Jun-Jie,Z.; *Nanoscale*., **2013**, *5*, 4015–4039.
    DOI: 10.1039/c3nr33849e

21. Hiromi, A.; Koichi, M.; Atul, S.; Akira, T.; *Energy & Fuels,* **2003,** *17* (5), 1244–1250.
    DOI: 10.1021/ef020265u

22. Spataru, N.; Sarada, B.V.; Tryk, D.A.; Fujishima, A.; *Electroanalysis*, **2002**, *14*, 721-728.
    DOI: 10.1002/1521-4109(200206)14:11

23. Pizzariello, A.; Svorc, J.; Stredansky, M.; Miertus, S.; *J. Sci. Food Agric.,* **1999**, *79*, 1136-1140.
    DOI: 10.1002/(SICI)1097-0010(199906)79:8

24. Zhao, F.;Wang, F.; Zhao, W.; Zhou, J.; Liu, Y.; Zou, L.; Ye, B.; *Microchimica Acta*, **2011**, *174* (3), 383–390.
    DOI: 10.1007/s00604-011-0635-y

25. Summers, R.M.; Mohanty, S.K.; Gopishetty, S.; Subramanian, M.; *Microbial Biotechn,*, **2015**, *8(3)*, 369–378.
    DOI: 10.1111/1751-7915.12262

26. De Maria, C.A.B.; Moreira, R.F.A.; *Quim. Nova*., **2007**, *30*, 99-105.
    DOI: 10.1590/S0100-40422007000100021

27. Arinobu,T.; Hattori, H.; Kumazawa, T.; Lee, X.P.; Mizutani, Y.; Katase, T.;Kojima, S.; Omori, T.; Kaneko, R.; Ishii, A.; Seno, H.; *Forensic Toxicol.*, **2009,** *27*, 1-6.
     DOI: 10.1007/s11419-008-0058-6

28. Aranda, M.; Morlock, G.; *J. Chromatogr. Sci*., **2007**, *45*, 251-255.
     DOI: 10.1002/rcm.2949

29. Moriyasu, K.; Saito, M.; Nakazato, F.;Ishikawa, K.; Fujinuma, T.; Nishima, A.; Kunagi Tabei, K.; *HRC J. High Resolut. Chromatogr.*, **1997**, *20*, 456-468.
     DOI: 10.2478/s11532-011-0058-y

30. Alpdogan, G.; Karabina, K.; Sungur, S.; *Turk. J. Chem.*, **2002**, *26*, 295-302.
     DOI: 10.3923/pjn.2012.336.342

31. Zhao, Y.P.; Lunte, C.E.; *J. Chromatogr. B Biomed Sci Appl.* , **1997**, *628*, 265-274.
     DOI: 10.1097/pubmed/9061464

32. Sarath Babu, V.R.; Patraa, S.;Karantha, N.G.; Kumar, M.A.; Thakur, M.S.; *Anal. Chim. Acta*, **2007**, *582(2)*, 329–334.
     DOI: 10.1016/j.aca.2006.09.017

33. Emre, D.; Ozaltin, N.; *J. Chromatogr. B*, **2007**, 847(2), 126-132.
     DOI: 10.1016/j.jchromb.2006.09.036

34. Amini, A.; Barclay, V.; Rundlof, T.; Jonsson, S.; Karlsson, A.; Arvidsson, T.; *Chromatographia*., **2006**, *63*, 143-148.
     DOI: 10.1365/s10337-006-0726-9

35. Marcoux, L.S.; Prater, K.B.; Prater, B.G.; Adams, R.N.; *Anal. Chem.*, **1958,** *30*, 1576-1576.
     DOI: 10.1021/ac60230a047

36. Sanghavi, B.J.; Wolfbeis, O.S.; Hirsch, T.; Swami, N. S.; *Mikrochim Acta.,* **2015,** *182*, 1-41.
     DOI: 10.1007/s00604-014-1308-4

37. Parlak, O.; Turner, APF.; Tiwari, A.; *J. Mater. Chem. B*, **2015**, 3, 7434.
     DOI:10.1039/C5TB01355K

38. Ruquan, Y.; Changsheng, X.; Jian, L.; Zhiwei, P.; Kewei, H.; Zheng, Y.; Cook, C.P.; Samuel, L.G.; Chih-Chau, H.; Gedeng, R.; Gabriel, C.; Abdul-Rahman, O.R.; Mart, Angel A.; Tour, James M.; *Nat. communication,* **2013,** *4*:2943, 1-6.
     DOI: 10.1039/c5ra02961a

39. Manoj, B.; Narayanan, P.; *J. Minerals and Materials Characterization and Eng.,* **2013**, *1*, 39-43.
     DOI: 10.4172/2155-6199-1000306.

40. Hummers Jr., W. S.; Offeman. R. E.; *J. Am. Chem. Soc.*, **1958**, *80 (6),* 1339–1339.
     DOI: 10.1021/ja01539a017

41. Abdolhosseinzadeh, S.; Hamed, A.; Kim, H.S.; *Scientific Reports*, **2015**, *5*, 10160.
     DOI: 10.1038/srep10160

42. Martínez-Huitle, C. A.; Suely Fernandes, N.; Ferro, S.; De Battisti, A.; Quiroz, M. A.; *Diamond Related Materials,* **2010**, *19* (10), 1188.
     DOI: 10.1016/j.diamond.2010.05.004

43. Ly, S. Y.; Jung, Y. S.; Kim, M. H.; Han, I. K.; Jung, W. W.; Kim, H. S.; *Mikrochim. Acta,* **2004**, *146* (3–4), 207.
     DOI: 10.1007/s00604-004-0209-3

44. Zen, J. M.; Ting, Y. S.; Shih, Y.; Analyst (Lond.) **1998,** *123* (5), 1145.
     DOI: 10.1039/an/a708360b

45. Akyilmaz, E.; Turemis, M.; *Electrochim. Acta* **2010,** *55* (18), 5195.
     DOI: 10.1016/j.electacta.2010.04.038

46. Biuck, H.; Mehri, A.; Mohammad, H.; Pournaghi-Azar, A.; *Chinese Journal of Catalysis*, **2012**, *33 (11*), 1783-1790.
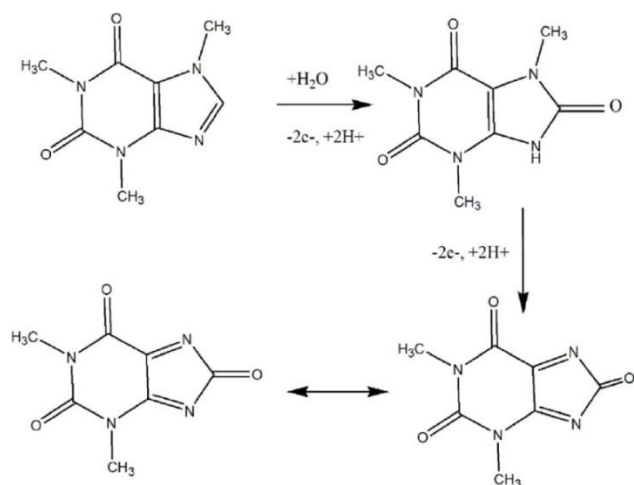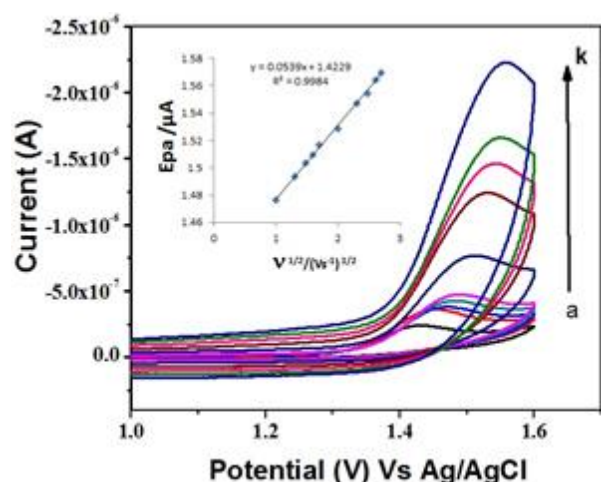   **DOI:** 10.1016/S1872-2067(11)60438-5

Supporting Information

Fig. S1. Anodic oxidation of caffeine.

Fig. S2 CVs of (GME) in the presence of 1.0 x10⁻⁵ M caffeine with different scan rate of 10mV to 500mV. Inserts E_{pa} Vs Square root of scan rates.

Effect of scan rate

To obtain the kinetic parameters of caffeine at GME, the scan rate effect was investigated by cyclic voltammetry **(Fig. 5a)**. Only oxidation peaks were observed, indicating that the oxidation of caffeine was a totally irreversible electrode process. Along with the increase of the scan rate, the oxidation peak currents of caffeine increased gradually, and the relationship of the oxidation peak current with the square root of the scan rate were established with linear regression equations (Eqn. (2)). With increasing scan rate, the anodic peak potential at the GME slightly shifted positively. For an irreversible system, at a higher scan rate the relationship between E_{pa} (absolute potential at the oxidation peak) and ln ν should submit to the equation (2). In this work, the linear regression equation was expressed as follows: E= 1.45 + 0.093 ln ν (E is absolute potential in V, ν is in V s⁻¹, and R = 0.998), thus RT/2(1 − α) nF = 0.0279, where T is absolute temperature (K), a is the electron transfer coefficient, and nF is the number of electrons × Faraday constant). Letting (n = 2, 1) was estimated to be 0.73.
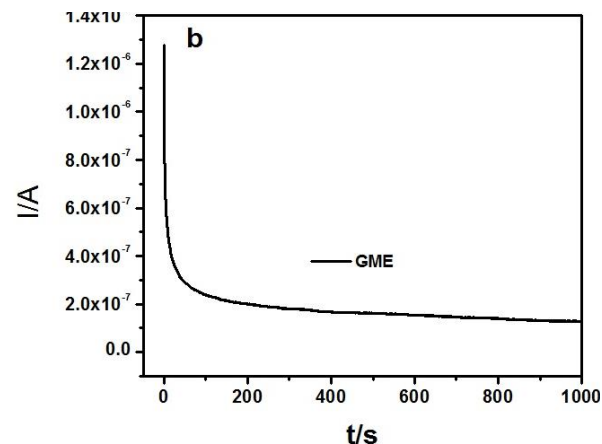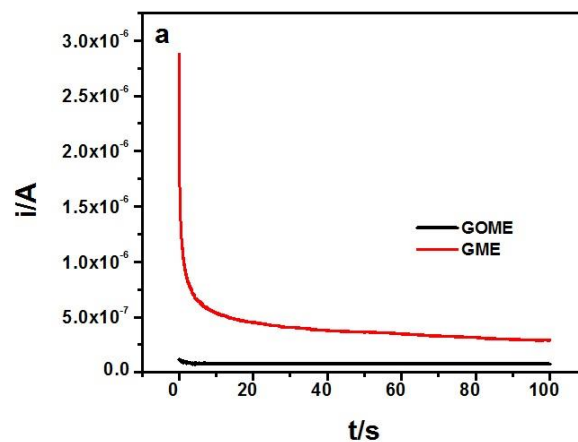

Fig. S3. (a) Chronoamperograms showing the variation of current with time at the caffeine-oxidation potential for the GOME and GME electrodes. (b) Chronoamperogram showing the variation of current with time for the GME electrode.

Table 3. Determination of the results from caffeine in spiked cola beverage (n = 5).

Added (mol L⁻¹)	Expected (mol L⁻¹)	Found (mol L⁻¹)	Average recovery (%)	Ref. value (mol L⁻¹)*	Ref. value (mol L⁻¹)*
0	-	2.0×10⁻⁵	-	2.05×10⁻⁵	1.99×10⁻⁵
1.0×10⁻⁵	3.0×10⁻⁵	3.07×10⁻⁵	102.3		
8.0×10⁻⁶	2.8×10⁻⁵	2.78×10⁻⁵	101.4		
5.0×10⁻⁶	2.5×10⁻⁵	2.48×10⁻⁵	98.6		
1.0×10⁻⁶	2.1×10⁻⁵	2.09×10⁻⁵	97.8		

Stability of electrode

In this chronoamperograms were recorded for the graphene oxide and reduced graphene oxide were show in Figure S3. Chronoamperometry was employed to exam the action of these two electrodes. The electrode potential was stepped to the oxidation potential of caffeine in each case. For the GMEs, the steady-state current remained at a higher value than for the GOME and GME. In the case of GOME and GME, the currents reached near-zero values within 13 s. However, for the GMEs, a constant current of 0.2 mA was detected even after 100 s and 1000s (Figure (a) and (b)). This shows that GMEs should be better catalytic electrodes for practical applications. Figure b

was observed by chronoamperometry that currents were sustained for a longer period in the case of GMEs. This may be the reason for the high catalytic activity of these electrodes. Such as GMEs were having a large surface area and high catalytic currents are desirable for applications.

Table 4. Evaluation with other electrochemical techniques for detection of caffeine.

Methods/reagent(s) used	Analytical range (μ mol L⁻¹)	LODs (μ mol L⁻¹)	References
Nafion-BDD electrode	0.2-12	1	42
Graphite pencil electrode	Up to 2574.8	47.4	43
Nafion-ruthenium oxide pyrochlore CME	5.0–200	2	44
Carbon paste electrode	1	0.35	45
Nafion/MWCNT	125.2	0.23	46
GME/carbon paste electrode	0.2 -120	0.10	This work